

NFN - Nationales Forschungsnetzwerk

Geometry + Simulation

<http://www.gs.jku.at>



Stabilized space-time finite element methods of parabolic evolution problems

Ioannis Touloupoulos

G+S Report No. 58

May 2017

FWF

Der Wissenschaftsfonds.

JKU
JOHANNES KEPLER
UNIVERSITY LINZ

Stabilized space-time finite element methods of parabolic evolution problems

Ioannis Touloupoulos¹

¹ Johann Radon Institute for Computational and Applied Mathematics (RICAM),
Austrian Academy of Sciences
Altenbergerstr. 69, A-4040 Linz, Austria,
`ioannis.touloupoulos@ricam.oeaw.ac.at`

Abstract. In this paper, a stabilized space-time finite element method for solving linear parabolic evolution problems is analyzed. The proposed method is developed on a base of a space-time variational setting, that helps on the simultaneous and unified discretization in space and time by finite element techniques. Stabilization terms are constructed by means of classical bubble spaces. Stability of the discrete problem with respect to a associated mesh dependent norm is proved, and a priori discretization error estimates are presented. Numerical examples confirm the theoretical estimates.

Key words: Parabolic initial-boundary value problems, space-time finite element methods, bubble stabilization, optimal convergence rates.

1 Introduction

Parabolic evolution equations are used to describe numerous physical phenomena, as for example heat transfer. The traditional methods for parabolic problems apply usually a separated method for the time discretization, e.g., implicit Runge-Kutta methods. Last decades, efficient discontinuous Galerkin finite element methods (DGFEM) have been presented for the time discretization of parabolic problems, see, e.g., an analysis for Galerkin time-stepping methods in [15], [12], [1], we also refer to the monograph [29]. Adaptive algorithms based on a posteriori error estimates have also been presented and successfully tested for linear and nonlinear problems, see e.g., [13], [14] and the references therein. In [27] and [10], space-time adaptive wavelet methods for parabolic evolution problems have been studied. Also in the literature, p and hp finite element methods for parabolic problems have been presented, see [5], [6].

Another approach that has been followed is the derivation of space-time finite element methods based on appropriate space-time variational setting. The basic idea is to consider the time variable t as just another variable, lets say x_{d+1} , if we consider that $x = (x_1, \dots, x_d)$ are the spatial variables. In that way, the time derivative, which appears in the parabolic PDE model, plays the role of a convection term in the time direction x_{d+1} . Multiplying the given parabolic problem by a space-time test function and applying integration by parts we can derive the weak space-time formulation. The derived weak formulation helps on the unified space-time discretization by finite element techniques, this means that we discretize the problem in space and in time by using a common finite element space. In this spirit in [21], space-time finite element methods have been developed for elastodynamics. In particular, the method uses discontinuous Galerkin techniques for the time discretization and incorporates Petrov-Galerkin techniques, see [22], to ensure stability. Stream line diffusion techniques that are presented in [22], have been also used for developing space-time finite element methods for conservation laws and fluid flow problems, see e.g., [20], [19] and the references there. In [2, 3], the stability of Petrov-Galerkin discretizations of parabolic problems have been studied and stable space-time trial and test functions have been proposed. In [28] conforming space-time finite element approximations to parabolic problems have been investigated. In [24], upwind-stabilized single-patch space-time Isogeometric analysis (IgA) schemes for parabolic evolution problems are proposed. In [25], the authors based on [24], analysed a time discontinuous Galerkin multipatch (IgA) scheme and demonstrated the efficiency of a space-time solver implemented on a parallel environment.

In this paper, we focus on the model problem $\partial_t u - \kappa \Delta u = f$, with appropriate initial and boundary conditions, and the diffusivity parameter κ is taken to be positive and constant. We propose a new space-time finite element method, which is stabilized by introducing classical bubble spaces, see [9], [7], [26]. The bubble basis functions vanish on the edges of the mesh elements and in addition do not affect the continuity properties of the solution. By enriching in that way the underlying finite element space, the numerical solution consists of two components, where the first lives in the underlying finite element space, and the second lives in the bubble space. For developing our analysis, we are motivated and inspired by the subgrid scale stabilization techniques presented in [17], [18], for solving linear first order problems. There, the idea is to couple, the initial finite element space with subgrid scale spaces and to construct artificial diffusion terms in these new spaces. The artificial diffusion terms are added in the numerical scheme in order to ensure stability. The innovation in our approach is that, instead of using subgrid spaces on different meshes, we use bubble spaces and the artificial diffusion terms are formed in these spaces. In addition here, in the bubble diffusion terms, we include a positive parameter θ , that can control the strength of the artificial diffusivity in the scheme. We prove stability of the discrete problem with respect to the produced norm, which is a mesh depended norm. Also, optimal error estimates for the full numerical solution containing the bubble component are shown. These error estimates are not affected by the choice of θ . Furthermore, we point out that during the discretization error analysis, we give analytically the dependence of the several appearing constants with respect to the diffusivity parameter κ . At the end, this helps us to have a more complete idea, about the convergence properties of the numerical solution, when the mesh size h is close to the value of κ . In Section 5, we perform tests where h and κ are very close.

The paper is structured as follows. In Section 2, the model parabolic problem is presented. In Section 3, we formulate the stabilized space-time finite element scheme. In Section 4, we present the error analysis and derive the error estimates. We discuss numerical examples in Section 5. The paper closes with the conclusions.

2 The model problem

2.1 Preliminaries

Let Ω be a bounded Lipschitz domain in \mathbb{R}^d , $d \geq 1$. Let $\boldsymbol{\alpha} = (\alpha_1, \dots, \alpha_d)$ be a multi-index of non-negative integers $\alpha_1, \dots, \alpha_d$ with degree $|\boldsymbol{\alpha}| = \sum_{j=1}^d \alpha_j$. For any $\boldsymbol{\alpha}$, we define the differential operator $D_x^\boldsymbol{\alpha} = D_{x_1}^{\alpha_1} \dots D_{x_d}^{\alpha_d}$, with $D_{x_j} = \partial/\partial x_j$, $j = 1, \dots, d$. As usual, $L^2(\Omega)$ denotes the Sobolev space for which $\int_\Omega |\phi(x)|^2 dx < \infty$, endowed with the norm $\|\phi\|_{L^2(\Omega)} = \left(\int_\Omega |\phi(x)|^2 dx \right)^{\frac{1}{2}}$, and $L^\infty(\Omega)$ denotes the functions that are essentially bounded. Let ℓ be a non-negative integer, define

$$H^\ell(\Omega) = \{\phi \in L^2(\Omega) : D_x^\boldsymbol{\alpha} \phi \in L^2(\Omega), \text{ for all } |\boldsymbol{\alpha}| \leq \ell\},$$

the standard Sobolev spaces endowed with the following norms $\|\phi\|_{H^\ell(\Omega)} = \left(\sum_{0 \leq |\boldsymbol{\alpha}| \leq \ell} \|D_x^\boldsymbol{\alpha} \phi\|_{L^2(\Omega)}^2 \right)^{\frac{1}{2}}$, and by $H^{\frac{1}{2}}(\partial\Omega)$ we denote the trace space of $H^1(\Omega)$. Also we define the subspace $H_0^1(\Omega)$ of $H^1(\Omega)$

$$H_0^1(\Omega) = \{\phi \in H^1(\Omega) : \phi = 0 \text{ on } \partial\Omega\}.$$

Let $I = [0, T]$ with $T > 0$ be the time interval. For later use, we define the space-time cylinder $Q = \Omega \times (0, T)$ and its boundary parts $\Sigma = \partial\Omega \times (0, T)$, $\Sigma_T = \Omega \times \{T\}$ and $\Sigma_0 = \Omega \times \{0\}$, see an illustration Fig. 1(a). We denote the gradient by $\nabla u = (\nabla_x u, \partial_t u)$, where $\nabla_x u$ is the gradient with respect to the spatial variables. Similarly we denote by $n = (n_x, n_t)$ the normal component on ∂Q , with n_x the components related to space direction and n_t the component related to time direction. Let ℓ, m be positive integers, for functions defined in Q , we define the Sobolev spaces

$$H^{\ell, m}(Q) = \{\phi \in L^2(Q) : D_x^\boldsymbol{\alpha} \phi \in L^2(Q) \text{ with } 0 \leq |\boldsymbol{\alpha}| \leq \ell, \text{ and } \partial_t^i \phi \in L^2(Q), i = 1, \dots, m\} \quad (2.1a)$$

and the subspaces

$$H_0^{1,0}(Q) = \{\phi \in L^2(Q) : \nabla_x \phi \in [L^2(Q)]^d, \phi = 0 \text{ on } \Sigma\}, \quad (2.1b)$$

$$H_{0,\bar{0}}^{1,1}(Q) = \{\phi \in L^2(Q) : \nabla_x \phi \in [L^2(Q)]^d, \partial_t \phi \in L^2(Q), \phi = 0 \text{ on } \Sigma, \phi = 0 \text{ on } \Sigma_T\}. \quad (2.1c)$$

For a function $\phi \in H^{\ell,m}(Q)$ with $\ell, m \geq 1$, we define the norms and the seminorms

$$\|\phi\|_{H^{\ell,m}(Q)} := \left(\sum_{|\alpha| \leq \ell} \|D^\alpha \phi\|_{L^2(Q)}^2 + \sum_{i=0}^m \|\partial_t^i \phi\|_{L^2(Q)}^2 \right)^{\frac{1}{2}}, \quad (2.2a)$$

$$|\phi|_{H^{\ell,m}(Q)} := \left(\sum_{|\alpha| = \ell} \|D^\alpha \phi\|_{L^2(Q)}^2 + \|\partial_t^m \phi\|_{L^2(Q)}^2 \right)^{\frac{1}{2}}. \quad (2.2b)$$

We recall Hölder's and Young's inequalities

$$\left| \int_Q uv \, dx \right| \leq \|u\|_{L^2(Q)} \|v\|_{L^2(Q)} \quad \text{and} \quad \left| \int_Q uv \, dx \right| \leq \frac{\epsilon}{2} \|u\|_{L^2(Q)}^2 + \frac{1}{2\epsilon} \|v\|_{L^2(Q)}^2, \quad (2.3)$$

that hold for all $u \in L^2(Q)$ and $v \in L^2(Q)$ and for any fixed $\epsilon \in (0, \infty)$.

We will use the following Poincaré's inequality: Let $\Omega \subset \mathbb{R}^d$, $d = 1, 2, \dots$ be a bounded rectangular domain and let $\Gamma \subset \partial\Omega$ with $|\Gamma| > 0$. For simplicity we assume that Γ lies on the plane with $x_1 = 0$. Let $v \in C^\infty(\Omega)$ and $v(x_\Gamma) = 0$ for all $x_\Gamma \in \Gamma$. For any interior point $x = (x_1, \dots, x_d)$, we have

$$v(x_1, \dots, x_d) = v(x_\Gamma) + \int_{x_{\Gamma,1}}^{x_1} \frac{\partial v}{\partial x_1}(\tau, x_2, \dots, x_d) \, d\tau. \quad (2.4)$$

The first inequality in (2.3) yields

$$(v(x_1, \dots, x_d))^2 = \left(\int_{x_{\Gamma,1}}^{x_1} \frac{\partial v}{\partial x_1}(\tau, x_2, \dots, x_d) \, d\tau \right)^2 \leq C_\Omega \int_{x_{\Gamma,1}}^{x_1} \left| \frac{\partial v}{\partial x_1}(\tau, x_2, \dots, x_d) \right|^2 \, d\tau, \quad (2.5)$$

where the constant C_Ω depends on the length of Ω . Integrating (2.5) over all Ω , we can obtain

$$\int_\Omega v^2(x) \, dx \leq C_\Omega^2 \int_\Omega (\partial_{x_1} v)^2 \, dx. \quad (2.6)$$

In what follows, positive constants c and C appearing in inequalities are generic constants which do not depend on the mesh-size h . In many cases, we will indicate on what may the constants depend for an easier understanding of the proofs. Frequently, we will write $a \sim b$ meaning that $ca \leq b \leq Ca$.

2.2 The model parabolic problem

In the space-time cylinder $\bar{Q} = \bar{\Omega} \times [0, T]$, we consider the initial boundary value problem

$$\begin{aligned} u_t - \kappa \Delta u &= f \text{ in } Q \quad \text{and} \\ u &= 0 \text{ on } \Sigma, \quad u(\cdot, 0) = u_0 \text{ on } \Sigma_0, \end{aligned} \quad (2.7)$$

as model problem, where the diffusivity parameter $0 < \kappa \leq 1$ is taken to be constant, $f : Q \rightarrow \mathbb{R}$, with $f \in L^2(Q)$, and $u_0 : \Omega \rightarrow \mathbb{R}$, with $u_0 \in L^2(\Omega)$ are given functions, and $u : \bar{Q} \rightarrow \mathbb{R}$ is the

unknown. The space-time weak formulation related to (2.7) has as follows: find $u \in H_0^{1,0}(Q)$ such that

$$\bar{a}(u, v) = \bar{l}(v), \text{ for all } v \in H_{0,0}^{1,1}(Q) \quad (2.8)$$

with

$$\bar{a}(u, v) = - \int_Q u(x, t) \partial_t v(x, t) dx dt + \kappa \int_Q \nabla_x u(x, t) \cdot \nabla_x v(x, t) dx dt, \quad (2.9)$$

$$\bar{l}(v) = \int_Q f(x, t) v(x, t) dx dt + \int_Q u_0(x) v(x, 0) dx. \quad (2.10)$$

For simplicity, we only consider homogeneous Dirichlet boundary conditions on Σ and $u_0 = 0$. However, the analysis presented in our paper can easily be generalized to other constellations of boundary conditions. The variational problem (2.11) is known to have a unique weak solution, see [23] and in [30] for a more comprehensive analysis for existence and uniqueness results.

Assumption 2.1 *We assume that the solution u of (2.11) belongs to $V_{0,0} = H_{0,0}^{1,1}(Q) \cap H^{\ell,m}(Q)$ with some $\ell \geq 2$ and $m > 1$.*

Under Assumption 2.1, by applying integration by parts, we can show that the weak solution satisfies the form

$$a(u, v) = l(v), \text{ for all } v \in H_{0,0}^{1,1}(Q), \quad \text{with} \quad (2.11a)$$

$$a(u, v) = \int_Q \partial_t u(x, t) v(x, t) dx dt + \kappa \int_Q \nabla_x u(x, t) \cdot \nabla_x v(x, t) dx dt, \quad (2.11b)$$

$$l(v) = \int_Q f(x, t) v(x, t) dx dt. \quad (2.11c)$$

3 The discrete problem

3.1 The stabilized scheme

Let $T_h(Q)$ be a partition of space-time domain Q into triangular (or quadrilateral elements), that is $\bar{Q} = \cup_{E \in T_h} E$, see Fig 1(a). We denote by h_E the diameter of $E \in T_h(Q)$ and the mesh size is defined as $h = \max_E \{h_E\}$. We assume that $T_h(Q)$ is quasi-uniform, i.e., there exist a positive constant C_{um} such that $h_E \leq h \leq C_{um} h_E$ for all $E \in T_h(Q)$.

Associated with $T_h(Q)$, we define the finite element subspace V_{h0} of $H_{0,0}^{1,1}(Q)$, consisting of continuous functions in space and in time, by

$$V_{h0} = \{v_h \in H_{0,0}^{1,1}(Q) : v_h|_E \in \mathbb{P}^{p-1}(E), \text{ for every } E \in T_h(Q)\}, \quad (3.1)$$

where $\mathbb{P}^{p-1}(E)$ is the polynomial space of total degree $p = 1$, see e.g., [8, 11, 16].

The usual finite element approximation of (2.11) is to find $u_h \in V_{h0}$ such that

$$a(u_h, v_h) = (f, v_h), \quad \forall v_h \in V_{h0}. \quad (3.2)$$

It is known, that when κ is small, the coercivity properties of (2.11) can not ensure that the usual finite element scheme given in (3.2) performs well. Thus, we introduce the a larger finite subspace $V_{h,b}$ of $H_{0,0}^{1,1}(Q)$ that can be written as a direct sum as follows

$$V_{h,b} = \{v_h \in H_{0,0}^{1,1}(Q) : v_h|_E \in \mathbb{P}^1(E) \oplus V_B(E), \text{ for every } E \in T_h(Q)\}, \quad (3.3)$$

with $V_B(E) := V_B|_E$, where V_B denotes the space of bubble functions, that vanishing entirely on the boundary of the mesh elements and having exactly one degree of freedom in each $E \in T_h(Q)$.

For example, for triangular elements is spanned by a cubic functions $V_B := \{v^b \in H_0^1(Q) : v^b|_E = C_E \lambda_1 \lambda_2 \lambda_3\}$, where $\lambda_i, i = 1, 2, 3$ are linear polynomials vanishing on one side of ∂E and taking the value one at the opposite vertex. The constant C_E is chosen such that $\max_{x \in E} v^b(x) = 1$. Every bubble basis function $\phi \in V_B(E)$ satisfies, (i) $\phi(x) > 0$ for $x \in E$ and (ii) $\phi(x) = 0$ for $x \in \partial E$, (iii) $\int_E \phi^2(x) dx = C_E h_E^2$, with C_E depending on the uniformity of T_h but is interdependent of h_E . An illustration of bubble functions on two-dimensional elements is presented in Fig. 1(b) and (c). Based on $V_{h,b}$ defined in (3.3), any $v_h \in V_{h,b}$ can be decomposed into two parts, i.e., $v_h = v_h^1 + v_h^b$ with $v_h^1 \in V_{h0}$ and $v_h^b \in V_B$. In view of these, we introduce the discrete problem: find $u_h \in V_{h,b}$ such that

$$a(u_h, v_h) + b_h(u_h^b, v_h^b) = (f, v_h), \quad \forall v_h \in V_{h,b}, \quad (3.4a)$$

where

$$a(w, v) = \int_Q \partial_t w v dx dt + \kappa \int_Q \nabla_x w \cdot \nabla_x v dx dt, \quad (3.4b)$$

$$b_h(w^b, v^b) = \theta h \int_Q \partial_t w^b \partial_t v^b dx dt,$$

with $\theta > 0$ a positive constant, which will be determined later. We recall the following inverse estimate and the scaled trace inequality, where the proofs can be found in [8].

Lemma 3.1. *There exist constants $c_{inv}, c_{trac} > 0$ independent of h such that*

$$\|\nabla v_h\|_{L^2(Q)} \leq c_{inv} h^{-1} \|v_h\|_{L^2(Q)}, \quad v_h \in V_{h,b}, \quad (3.5)$$

$$\|v\|_{L^2(\partial Q)} \leq c_{trac} h^{\frac{-1}{2}} (\|v\|_{L^2(Q)} + h \|\nabla v\|_{L^2(Q)}), \quad v \in H^1(Q). \quad (3.6)$$

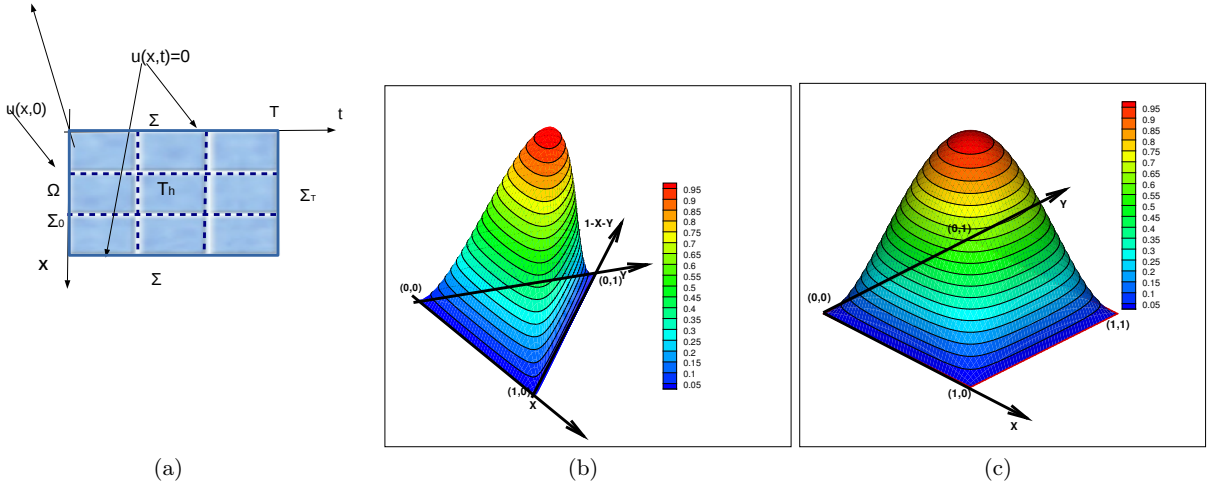


Fig. 1: (a) The space-time domain Q with the boundary parts and its mesh $T_h(Q)$. (b) The bubble function on the reference triangular mesh element. (c) The bubble function on the reference rectangular element.

For convenience, we introduce the discrete bilinear form

$$a_h(u_h, v_h) = a(u_h, v_h) + b_h(u_h^b, v_h^b), \quad (3.7)$$

and the mesh dependent norm

$$\|v_h\|_h = \left(\kappa \|\nabla_x v_h\|_{L^2(Q)}^2 + \theta h \|\partial_t v_h^b\|_{L^2(Q)}^2 + \frac{1}{2} \|v_h\|_{L^2(\Sigma_T)}^2 \right)^{\frac{1}{2}}. \quad (3.8)$$

Lemma 3.2. *The discrete form $a_h(\cdot, \cdot) : V_{h,b} \times V_{h,b} \rightarrow \mathbb{R}$ defined in (3.7), is $V_{h,b}$ -coercive with respect the norm $\|\cdot\|_h$, i.e.,*

$$a_h(v_h, v_h) \geq C_s \|v_h\|_h^2, \quad \forall v_h \in V_{h,b}. \quad (3.9)$$

Proof. Let $v_h \in V_h$. Since $v_h(x, 0) = 0$ and $n_t|_\Sigma = 0$, it follows by Green's formula

$$\begin{aligned} \int_Q \partial_t v_h v_h + v_h \partial_t v_h dx dt &= \int_{\partial Q} n_t v_h^2 ds, \text{ that} \\ \int_Q \partial_t v_h v_h dx dt &= \frac{1}{2} \int_Q \partial_t v_h^2 dx dt = \frac{1}{2} \int_{\Sigma_T} v_h^2 ds - \frac{1}{2} \int_{\Sigma_0} v_h^2 ds = \frac{1}{2} \|v_h\|_{L^2(\Sigma_T)}^2. \end{aligned} \quad (3.10)$$

The definition of a_h and (3.10) imply

$$\begin{aligned} a_h(v_h, v_h) &= \int_Q \frac{1}{2} \partial_t v_h^2 + \theta h (\partial_t v_h^b)^2 + \kappa |\nabla_x v_h|^2 dx dt \\ &= \frac{1}{2} \|v_h\|_{L^2(\Sigma_T)}^2 + \kappa \|\nabla_x v_h\|_{L^2(Q)}^2 + \theta h \|\partial_t v_h^b\|_{L^2(Q)}^2, \end{aligned} \quad (3.11)$$

which is (3.9) with $C_s = 1$ and this completes the proof. \blacksquare

Proposition 3.1. *Let u_h be a solution given by (3.4). Then there is a $C_\kappa > 0$ such that the solution u_h satisfies the following a priori estimate*

$$\|u_h\|_h \leq C_\kappa \|f\|_{L^2(Q)}. \quad (3.12)$$

Proof. Using $u_h \in V_{h,b}$ as a test function in (3.4), and utilizing (2.3) together with Poincare inequality (2.6), we successively obtain

$$\begin{aligned} a_h(u_h, u_h) &\leq \frac{1}{\kappa^{\frac{1}{2}}} \left| \int_Q \kappa^{\frac{1}{2}} f u_h dx dt \right| \leq \frac{1}{\kappa^{\frac{1}{2}}} \|f\|_{L^2(Q)} \|\kappa^{\frac{1}{2}} \nabla_x u_h\|_{L^2(Q)} \leq \\ &\frac{1}{\kappa} \|f\|_{L^2(Q)} (\kappa \|\nabla_x u_h\|_{L^2(Q)}^2 + \frac{1}{2} \|u_h\|_{L^2(\Sigma_T)}^2 + \theta h \|\partial_t u_h^b\|_{L^2(Q)}^2)^{\frac{1}{2}}, \end{aligned} \quad (3.13)$$

where, we have previously used that $\kappa \leq 1$. Setting $C_\kappa = \frac{1}{\kappa}$ we get (3.12). \blacksquare

A direct result of (3.12) and (3.9) is the following corollary.

Corollary 3.1. *The discrete problem defined in (3.4) is well posed, i.e., it has a unique solution which satisfies the stability estimate (3.9).*

Next, we show the boundedness of $a(\cdot, \cdot)$ on $V_{0,0} \times V_{h,b}$. We define the norms

$$\|v\|_{h,*} = (\kappa \|\nabla_x v\|_{L^2(Q)}^2 + \theta h \|\partial_t v\|_{L^2(Q)}^2 + \frac{1}{2} \|v\|_{L^2(\Sigma_T)}^2)^{\frac{1}{2}}. \quad (3.14a)$$

$$\|v\|_{h,V} = (\kappa \|\nabla_x v\|_{L^2(Q)}^2 + \theta h \|\partial_t v\|_{L^2(Q)}^2 + \frac{1}{2} \|v\|_{L^2(\Sigma_T)}^2 + (\theta h)^{-1} \|v\|_{L^2(Q)}^2)^{\frac{1}{2}}. \quad (3.14b)$$

Lemma 3.3. *There is a constant $C_b(\kappa, \theta, h) > 0$ such that*

$$|a(u, v_h)| \leq C_b(\kappa, \theta, h) \|u\|_{h,V} \|v_h\|_h, \quad \forall (u, v_h) \in (V_{0,0} \times V_{h,b}) \quad (3.15)$$

Proof. Let $v_h = v_h^1 + v_h^b \in V_{h,b}$. We treat every term of the form $a(\cdot, \cdot)$ separately. We apply integration by parts and (2.3) to infer

$$\begin{aligned}
\int_Q \partial_t u v_h^1 dx dt &= - \int_Q u \partial_t v_h dx dt + \int_{\Sigma_T} u v_h d\sigma \\
&\leq ((\theta h)^{-1} \|u\|_{L^2(Q)}^2)^{\frac{1}{2}} ((\theta h) \|\partial_t v_h\|_{L^2(Q)}^2)^{\frac{1}{2}} + \|u\|_{L^2(\Sigma_T)} \|v_h^1\|_{L^2(\Sigma_T)} \\
&\stackrel{(3.5)}{\leq} ((\theta h)^{-1} \|u\|_{L^2(Q)}^2)^{\frac{1}{2}} \left(\frac{c_1 \theta h}{h^2 \kappa} \kappa \|v_h\|_{L^2(Q)}^2 \right)^{\frac{1}{2}} + 2 \left(\frac{1}{2} \|u\|_{L^2(\Sigma_T)}^2 \right)^{\frac{1}{2}} \left(\frac{1}{2} \|v_h\|_{L^2(\Sigma_T)}^2 \right)^{\frac{1}{2}} \\
&\stackrel{(2.6)}{\leq} ((\theta h)^{-1} \|u\|_{L^2(Q)}^2)^{\frac{1}{2}} (c_2 \theta (\kappa h)^{-1})^{\frac{1}{2}} \left(\kappa \|\nabla_x v_h\|_{L^2(Q)}^2 + \theta h \|\partial_t v_h^b\|_{L^2(Q)}^2 + \frac{1}{2} \|v_h\|_{L^2(\Sigma_T)}^2 \right)^{\frac{1}{2}} \\
&\quad + 2 \|u\|_{L^2(\Sigma_T)} \left(\kappa \|\nabla_x v_h\|_{L^2(Q)}^2 + \theta h \|\partial_t v_h^b\|_{L^2(Q)}^2 + \frac{1}{2} \|v_h\|_{L^2(\Sigma_T)}^2 \right)^{\frac{1}{2}} \\
&\leq (c_2 \theta (\kappa h)^{-1})^{\frac{1}{2}} \|u\|_{h,V} \|v_h\|_h + 2 \|u\|_{h,V} \|v_h\|_h \leq c_3 (\theta (\kappa h)^{-1} + 1)^{\frac{1}{2}} \|u\|_{h,V} \|v_h\|_h,
\end{aligned} \tag{3.16}$$

where c_3 depends on the constants appearing in (3.5) and (2.6). Similarly for the second term, applying (2.3), we get

$$\int_Q \kappa^{\frac{1}{2}} \nabla_x u \cdot \kappa^{\frac{1}{2}} \nabla_x v_h dx dt \leq (\kappa \|\nabla_x u\|_{L^2(Q)}^2)^{\frac{1}{2}} (\kappa \|\nabla_x v_h\|_{L^2(Q)}^2)^{\frac{1}{2}} \leq \|u\|_{h,V} \|v_h\|_h. \tag{3.17}$$

Combining all the bounds above and setting $C_b(\kappa, \theta, h) = 2c_3(\theta(\kappa h)^{-1} + 1)^{\frac{1}{2}}$, we can derive the desired result. \blacksquare

4 Error analysis

Lemma 4.1 (weak consistency). *Let u_h the solution given by (3.4) and u the continuous solution given by (2.11), and furthermore let $z_h \in V_{h,b}$ and $v_h^1 \in V_{h0}$. Then*

$$a_h(u_h, z_h) = a(u, z_h), \quad \text{and} \tag{4.1a}$$

$$a_h(v_h^1, z_h) = a(v_h^1, z_h). \tag{4.1b}$$

Proof. For the first relation, we recall the problems (2.11) and (3.4) and directly have

$$a_h(u_h, z_h) = (f, z_h) = a(u, z_h). \tag{4.2}$$

For the second relation, we observe that $b_h(v_h^1, z_h) = 0$ for any $v_h^1 \in V_{h0}$ and the assertion directly follows. \blacksquare

Proposition 4.1. *Let u solve (2.11) and u_h solve (3.4) and $z_h^1 \in V_{h0}$. Under Assumption 2.1, there exist a c , independent of h such that*

$$(\|u - u_h\|_{L^2(\Sigma_T)}^2 + \kappa \|\nabla_x u - \nabla_x u_h\|_{L^2(Q)}^2 + \theta h \|\partial_t u_h^b\|_{L^2(Q)}^2) \leq \frac{c}{\kappa} (\|\nabla u - \nabla z_h^1\|_{L^2(Q)}^2 + \|u - z_h^1\|_{L^2(\Sigma_T)}^2). \tag{4.3}$$

Proof. Let an arbitrary $z_h^1 \in V_{h0}$. By (4.1) and by subtracting similar terms, we have that

$$\begin{aligned}
&\int_Q (\partial_t u_h - \partial_t z_h^1) \phi_h + \kappa \int_Q \nabla_x (u_h - z_h^1) \cdot \nabla_x \phi_h + \theta h \int_Q \partial_t u_h^b \partial_t \phi_h^b \\
&= \int_Q (\partial_t u - \partial_t z_h^1) \phi_h + \kappa \int_Q \nabla_x (u - z_h^1) \cdot \nabla_x \phi_h, \quad \forall \phi_h \in V_{h,b}.
\end{aligned} \tag{4.4}$$

Setting above $\phi_h = u_h^1 + u_h^b - z_h^1$ and applying integration by parts on the first term on the left side, we have

$$\begin{aligned} & \int_{\Sigma_T} |\partial_t u_h - \partial_t z_h^1|^2 d\sigma + \kappa \int_Q |\nabla_x(u_h - z_h^1)|^2 dx dt + \theta h \int_Q |\partial_t u_h^b|^2 dx dt \\ & \leq \left(\frac{1}{\kappa} \int_Q |\partial_t u - \partial_t z_h^1|^2\right)^{\frac{1}{2}} \left(\kappa \int_Q |u_h - z_h^1|^2\right)^{\frac{1}{2}} + \left(\int_Q \kappa |\nabla_x(u - z_h^1)|^2\right)^{\frac{1}{2}} \left(\int_Q \kappa |\nabla_x(u_h - z_h^1)|^2\right)^{\frac{1}{2}}, \end{aligned} \quad (4.5)$$

and by applying (2.3) and (2.4) on the right hand side, yields

$$\begin{aligned} & \|u_h - z_h^1\|_{L^2(\Sigma_T)}^2 + \kappa \|\nabla_x u_h - \nabla_x z_h^1\|_{L^2(Q)}^2 + \theta h \|\partial_t u_h^b\|_{L^2(Q)}^2 \leq \frac{1}{c_\epsilon \kappa} \|\partial_t u - \partial_t z_h^1\|_{L^2(Q)}^2 + \\ & c_\epsilon \kappa \|\nabla_x u_h - \nabla_x z_h^1\|_{L^2(Q)}^2 + \frac{\kappa}{c_\epsilon} \|\nabla_x u - \nabla_x z_h^1\|_{L^2(Q)}^2 + c_\epsilon \kappa \|\nabla_x u_h - \nabla_x z_h^1\|_{L^2(Q)}^2. \end{aligned} \quad (4.6)$$

Gathering the same terms and setting $0 < c_\epsilon < \frac{1}{2}$, we get

$$\begin{aligned} & (1 - 2c_\epsilon) \left(\|u_h - z_h^1\|_{L^2(\Sigma_T)}^2 + \kappa \|\nabla_x u_h - \nabla_x z_h^1\|_{L^2(Q)}^2 + \theta h \|\partial_t u_h^b\|_{L^2(Q)}^2 \right) \\ & \leq \frac{1}{c_\epsilon \kappa} \|\partial_t u - \partial_t z_h^1\|_{L^2(Q)}^2 + \frac{\kappa}{c_\epsilon} \|\nabla_x u - \nabla_x z_h^1\|_{L^2(Q)}^2 + \|u - z_h^1\|_{L^2(\Sigma_T)}^2. \end{aligned} \quad (4.7)$$

Using $0 < \kappa \leq 1$, applying triangle inequality and setting $c = \frac{1}{(1-2c_\epsilon)c_\epsilon}$, the assertion follows. \blacksquare

Below, we give the main error bound for the finite element solution $u_h \in V_{h,b}$.

Theorem 4.1. *Let u solve (2.11) and $u_h = u_h^1 - u_h^b$ solve (3.4). Under Assumption 2.1, there exist a $c_{*,V}$, depending on c_{inv} , such that*

$$\|u - u_h\|_{h,*} \leq c_{*,V} \left(1 + (\theta h \gamma^2(\kappa, \theta, h) + 1) \tilde{\gamma}(\kappa, \theta, h)\right)^{\frac{1}{2}} \|u - z_h^1\|_{h,V}, \quad \text{for } z_h^1 \in V_{h0}, \quad (4.8)$$

with $\gamma(\kappa, \theta, h) = \left(\frac{1}{(\theta h)^{\frac{1}{2}}} + \frac{c_{inv} \kappa^{\frac{1}{2}}}{h}\right)$ and $\tilde{\gamma}(\kappa, \theta, h) = [1 + (\theta h)^{\frac{1}{2}} \gamma(\kappa, \theta, h) + \theta h \gamma^2(\kappa, \theta, h)]$.

Proof. Let $z_h^1 \in V_{h0}$ and $\sigma_h = (u_h^1 + u_h^b) - z_h^1$. Using triangle inequality, we decompose the error as

$$\begin{aligned} & \frac{1}{2} \|u - u_h\|_{h,*}^2 = (\theta h) \|\partial_t u - \partial_t u_h\|_{L^2(Q)}^2 + \kappa \|\nabla_x u - \nabla_x u_h\|_{L^2(Q)}^2 + \frac{1}{2} \|u - u_h\|_{L^2(\Sigma_T)}^2 \\ & \leq \underbrace{(\theta h) \|\partial_t u - \partial_t z_h^1\|_{L^2(Q)}^2 + \kappa \|\nabla_x u - \nabla_x z_h^1\|_{L^2(Q)}^2}_{T_1} + \frac{1}{2} \|u - z_h^1\|_{L^2(\Sigma_T)}^2 + \underbrace{(\theta h) \|\partial_t u_h^1 - \partial_t z_h^1\|_{L^2(Q)}^2}_{T_2} \\ & \quad + \underbrace{(\theta h) \|\partial_t u_h^b - 0 \cdot \partial_t z_h^b\|_{L^2(Q)}^2 + \kappa \|\nabla_x u_h - \nabla_x z_h^1\|_{L^2(Q)}^2}_{T_3} + \frac{1}{2} \|u_h - z_h^1\|_{L^2(\Sigma_T)}^2 \\ & \leq \|u - z_h^1\|_{h,V}^2 + T_2 + \|\sigma_h\|_h^2, \end{aligned} \quad (4.9)$$

where we previously used that $T_1 := \|u - z_h^1\|_{h,*}^2 \leq \|u - z_h^1\|_{h,V}^2$ and $T_3 = \|\sigma_h\|_h^2$. We will proceed by giving bounds for every term appearing in (4.9). For doing this, we first show few auxiliary results. Let $v_h \in V_{h,b}$ and $\sigma_h^1 = u_h^1 - z_h^1$, then using (3.5), (3.7) and (4.1) and the fact that $0 < h, \theta, \kappa \leq 1$,

we can obtain that

$$\begin{aligned}
 \|\partial_t u_h^1 - \partial_t z_h^1\|_{L^2(Q)} &= \|\partial_t \sigma_h^1\|_{L^2(Q)} \leq \sup_{v_h \in V_{h,b}} \frac{\int_Q \partial_t ((u_h^1 + u_h^b) - z_h^1 - u_h^b) v_h \, dx \, dt}{\|v_h\|_{L^2(Q)}} \\
 &\leq \sup_{v_h \in V_{h,b}} \frac{-\left[\int_Q \partial_t u_h^b v_h + \kappa \nabla_x \sigma_h \cdot \nabla_x v_h + \theta h \partial_t u_h^b \partial_t v_h^b \, dx \, dt \right]}{\|v_h\|_{L^2(Q)}} \\
 &\quad + \sup_{v_h \in V_{h,b}} \frac{\left[\int_Q \partial_t (u - \partial_t z_h^1) v_h + \kappa \nabla_x (u - z_h^1) \cdot \nabla_x v_h + \right]}{\|v_h\|_{L^2(Q)}} \\
 &\leq \left(\frac{(\theta h)^{\frac{1}{2}}}{(\theta h)^{\frac{1}{2}}} \|\partial_t u_h^b\|_{L^2(Q)} + \frac{\theta^{\frac{1}{2}} (\theta h)^{\frac{1}{2}}}{h^{\frac{1}{2}}} \|\partial_t u_h^b\|_{L^2(Q)} \right) + \|\partial_t (u - z_h^1)\|_{L^2(Q)} \\
 &\quad + \kappa^{\frac{1}{2}} \left(\kappa^{\frac{1}{2}} \|\nabla_x (u - z_h^1)\|_{L^2(Q)} + \kappa^{\frac{1}{2}} \|\nabla_x \sigma_h\|_{L^2(Q)} \right) \sup_{v_h \in V_{h,b}} \frac{\|\nabla v_h\|_{L^2(Q)}}{\|v_h\|_{L^2(Q)}} \\
 &\leq \frac{1}{(\theta h)^{\frac{1}{2}}} (\theta h \|\partial_t u_h^b\|_{L^2(Q)}^2 + \kappa \|\nabla_x \sigma_h\|_{L^2(Q)}^2 + \frac{1}{2} \|\sigma_h\|_{L^2(\Sigma_T)}^2)^{\frac{1}{2}} \\
 &\quad + \frac{c_{inv} \kappa^{\frac{1}{2}}}{h} (\theta h \|\partial_t u_h^b\|_{L^2(Q)}^2 + \kappa \|\nabla_x \sigma_h\|_{L^2(Q)}^2 + \frac{1}{2} \|\sigma_h\|_{L^2(\Sigma_T)}^2)^{\frac{1}{2}} \\
 &\quad + \frac{c_{inv} \kappa^{\frac{1}{2}}}{h} \left(\kappa^{\frac{1}{2}} \|\nabla_x (u - z_h^1)\|_{L^2(Q)} \right) + \frac{(\theta h)^{\frac{1}{2}}}{(\theta h)^{\frac{1}{2}}} \|\partial_t (u - z_h^1)\|_{L^2(Q)} \\
 &\leq \left(\frac{1}{(\theta h)^{\frac{1}{2}}} + \frac{c_{inv} \kappa^{\frac{1}{2}}}{h} \right) \|\sigma_h\|_h + \left(\frac{1}{(\theta h)^{\frac{1}{2}}} + \frac{c_{inv} \kappa^{\frac{1}{2}}}{h} \right) \|u - z_h^1\|_{h,V} \\
 &\leq \gamma(\kappa, \theta, h) (\|u - z_h^1\|_{h,V} + \|\sigma_h\|_h).
 \end{aligned} \tag{4.10}$$

By using (4.10) and the relation

$$(\theta h)^{\frac{1}{2}} \|\partial_t u_h^1 - \partial_t z_h^1\|_{L^2(Q)} + (\theta h)^{\frac{1}{2}} \|\partial_t u_h^b - 0 \partial_t z_h^b\|_{L^2(Q)} \geq (\theta h)^{\frac{1}{2}} \|\partial_t (u_h^1 + u_h^b) - \partial_t z_h^1\|_{L^2(Q)}, \tag{4.11}$$

and observing that $(\theta h)^{\frac{1}{2}} \gamma(\kappa, \theta, h) \geq 1$, it follows that

$$(\theta h)^{\frac{1}{2}} \|\partial_t \sigma_h\|_{L^2(Q)} \leq 2(\theta h)^{\frac{1}{2}} \gamma(\kappa, \theta, h) (\|u - z_h^1\|_{h,V} + \|\sigma_h\|_h). \tag{4.12}$$

Furthermore, working as in the proof of (3.15) and using (4.18) and (2.3), we can find

$$\begin{aligned}
 a(u - z_h^1, \sigma_h) &= - \int_Q (u - z_h^1) \partial_t \sigma_h \, dx \, dt + \int_{\Sigma_T} (u - z_h^1) \sigma_h \, d\sigma + \int_Q \kappa^{\frac{1}{2}} \nabla_x (u - z_h^1) \cdot \kappa^{\frac{1}{2}} \nabla_x \sigma_h \, dx \, dt \\
 &\leq ((\theta h)^{-1} \|u - z_h^1\|_{L^2(Q)}^2)^{\frac{1}{2}} ((\theta h) \|\partial_t \sigma_h\|_{L^2(Q)}^2)^{\frac{1}{2}} + \|u - z_h^1\|_{L^2(\Sigma_T)} \|\sigma_h\|_{L^2(\Sigma_T)} \\
 &\quad + (\kappa \|\nabla_x (u - z_h^1)\|_{L^2(Q)}^2)^{\frac{1}{2}} (\kappa \|\nabla_x \sigma_h\|_{L^2(Q)}^2)^{\frac{1}{2}} \\
 &\leq 2 \|u - z_h^1\|_{h,V} (\theta h)^{\frac{1}{2}} \gamma(\kappa, \theta, h) (\|u - z_h^1\|_{h,V} + \|\sigma_h\|_h) + \|u - z_h^1\|_{h,V} \|\sigma_h\|_h \\
 &\leq 2(\theta h)^{\frac{1}{2}} \gamma(\kappa, \theta, h) \|u - z_h^1\|_{h,V}^2 + 4c_\varepsilon \theta h \gamma^2(\kappa, \theta, h) \|u - z_h^1\|_{h,V}^2 + \varepsilon \|\sigma_h\|_h^2 \\
 &\quad + c_\varepsilon \|u - z_h^1\|_{h,V}^2 + \varepsilon \|\sigma_h\|_h^2 \\
 &\leq 4c_\varepsilon \left[1 + (\theta h)^{\frac{1}{2}} \gamma(\kappa, \theta, h) + \theta h \gamma^2(\kappa, \theta, h) \right] \|u - z_h^1\|_{h,V}^2 + 2\varepsilon \|\sigma_h\|_h^2 \\
 &\leq 4c_\varepsilon \tilde{\gamma}(\kappa, \theta, h) \|u - z_h^1\|_{h,V}^2 + 2\varepsilon \|\sigma_h\|_h^2
 \end{aligned} \tag{4.13}$$

where we used that $0 < \varepsilon < \frac{1}{2}$ and $c_\varepsilon > 1$. Now, using the properties of $a_h(\cdot, \cdot)$ and $a(\cdot, \cdot)$, we have

$$C_s \|\sigma_h\|_h^2 \leq a_h(\sigma_h, \sigma_h) = a_h(u_h, \sigma_h) - a_h(z_h^1, \sigma_h) \stackrel{(4.1)}{=} a(u, \sigma_h) - a(z_h^1, \sigma_h) = a(u - z_h^1, \sigma_h), \tag{4.14}$$

and by (4.13) and by replacing $C_s = 1$, we obtain that

$$\|\sigma_h\|_h^2 \leq (1 - 2\varepsilon)^{-1} 4c_\varepsilon \tilde{\gamma}(\kappa, \theta, h) \|u - z_h^1\|_{h,V}^2 = \tilde{\gamma}_\varepsilon(\kappa, \theta, h) \|u - z_h^1\|_{h,V}^2. \quad (4.15)$$

Now, we can bound the terms in (4.9). Inequality (4.15) immediately implies

$$T_3 := \|\sigma_h\|_h^2 \leq \tilde{\gamma}_\varepsilon(\kappa, \theta, h) \|u - z_h^1\|_{h,V}^2. \quad (4.16)$$

Combining (4.10) and (4.15), we have that

$$\begin{aligned} T_2 &:= \theta h \|\partial_t u_h^1 - \partial_t z_h^1\|_{L^2(Q)}^2 \leq 2\theta h \gamma^2(\kappa, \theta, h) \left(\tilde{\gamma}_\varepsilon(\kappa, \theta, h) \|u - z_h^1\|_{h,V}^2 + \tilde{\gamma}_\varepsilon(\kappa, \theta, h) \|u - z_h^1\|_{h,V}^2 \right) \\ &= 4\theta h \gamma^2(\kappa, \theta, h) \tilde{\gamma}_\varepsilon(\kappa, \theta, h) \|u - z_h^1\|_{h,V}^2. \end{aligned} \quad (4.17)$$

Finally, gathering together the bounds (4.17) and (4.16), we obtain

$$\|u - u_h\|_{h,*}^2 \leq \|u - z_h\|_{h,V}^2 \left[1 + 4\theta h \gamma^2(\kappa, \theta, h) \tilde{\gamma}_\varepsilon(\kappa, \theta, h) + \tilde{\gamma}_\varepsilon(\kappa, \theta, h) \right]. \quad (4.18)$$

Setting $c_{*,V}^2 = 16(1 - 2\varepsilon)^{-1} c_\varepsilon$, we can derive estimate (4.8). ■

Remark 4.1. Let us consider a fixed $T_h(Q)$ and let us denote

$\mu(\kappa, \theta, h) = \left(1 + (\theta h \gamma^2(\kappa, \theta, h) + 1) \tilde{\gamma}(\kappa, \theta, h) \right)^{\frac{1}{2}}$, that is the factor appearing on the right hand side in (4.8). Then (i) for $\theta = 1$ and $\kappa > h$, it holds $\mu(\kappa, \theta, h) \sim h^{-\frac{1}{2}}$, (ii) for $\theta = 1$ and $\kappa \sim h$, it holds $\mu(\kappa, \theta, h) \sim 1$, (iii) for $\theta \sim h$ and $\kappa \sim h$, it holds $\mu(\kappa, \theta, h) \sim 1$.

Remark 4.2. In the proof of (4.8), we used (4.13). If instead of (4.13), we use (3.15), then we produce a corresponding new factor $\mu(\kappa, \theta, h)$, which has a suboptimal behavior wrt h . Precisely, the negative exponent of κ in $C_b(\kappa, \theta, h)$, i.e., see the factor $\theta(\kappa h)^{-1}$, makes the corresponding produced $\mu(\kappa, \theta, h)$ factor to be $\mathcal{O}(h^{-\frac{1}{2}})$.

Below, we recall some approximation estimates of the finite element space. For the proof we refer to [8].

Lemma 4.2. *Let s, m be integers such that $0 \leq m \leq 1 \leq s$ and let the space V_{h0} defined in (3.1). Then for every $v \in V := H_{0,0}^{1,1}(Q) \cap H^s(Q)$, there exist a linear interpolation operator $\pi_h v : V \rightarrow V_{h0}$ such that*

$$\|v - \pi_h v\|_{H^m(Q)} \leq c_{intp} h^{\min(p+1,s)-m} \|v\|_{H^s(Q)}, \quad (4.19)$$

where $c_{intp} = c(m, s, Q)$ and $p = 1$.

Lemma 4.3. *Let the space V_{h0} defined in (3.1). Let $s \geq 2$ be an integer, and let a function $v \in V := H_{0,0}^{1,1}(Q) \cap H^s(Q)$. There exist a linear interpolation operator $\pi_h v : V \rightarrow V_{h0}$ such that*

$$\|v - \pi_h v\|_{L^2(\Sigma_T)}^2 \leq c_1 h^{2r-1} \|v\|_{H^s(Q)}^2, \quad (4.20a)$$

$$\|v - \pi_h v\|_{h,*}^2 \leq c_2 h^{2r-1} (\kappa h^{-1} + \theta + 1) \|v\|_{H^s(Q)}^2, \quad (4.20b)$$

$$\|v - \pi_h v\|_{h,V}^2 \leq c_3 h^{2r-1} (\kappa h^{-1} + \theta + \theta^{-1} + 1) \|v\|_{H^s(Q)}^2, \quad (4.20c)$$

where $r = 2$ and c_1, c_2, c_3 depend on the constants appearing in (3.6) and in (4.19), but not on h and v .

Proof. Introducing the operator $\pi_h v$ of Lemma 4.2 and by applying (3.6) and (4.19), we have

$$\|u - \pi_h v\|_{L^2(\Sigma_T)}^2 \leq 2 c_{trac}^2 h^{-1} \left(\|v - \pi_h v\|_{L^2(Q)}^2 + h^2 \|\nabla(v - \pi_h v)\|_{L^2(Q)}^2 \right) \leq c_1 h^{2r-1} \|v\|_{H^s(Q)}^2. \quad (4.21)$$

In the same way, we have

$$\begin{aligned} \kappa \|\nabla_x(v - \pi_h v)\|_{L^2(Q)}^2 &\leq c_{intp} \kappa h^{2r-2} \|v\|_{H^2(Q)}^2, \\ \theta h \|\partial_t(v - \pi_h v)\|_{L^2(Q)}^2 &\leq c_{intp} \theta h^{2r-1} \|v\|_{H^2(Q)}^2, \\ (\theta h)^{-1} \|(v - \pi_h v)\|_{L^2(Q)}^2 &\leq c_{intp} \theta^{-1} h^{2r-1} \|v\|_{H^2(Q)}^2, \end{aligned} \quad (4.22)$$

Collecting the estimates (4.21) and (4.22), we easily obtain

$$\|v - \pi_h v\|_{h,V}^2 \leq c_3 (\kappa h^{2r-2} + \theta h^{2r-1} + \theta^{-1} h^{2r-1} + h^{2r-1}) \|v\|_{H^2(Q)}^2, \quad (4.23)$$

which is (4.20c). The estimate given in (4.20b) follows similarly. \blacksquare

Remark 4.3. The interpolation estimates presented in (4.20) have been derived for linear polynomial spaces, see (3.1). Analogous estimates can be derived for higher polynomial spaces. In that case we set $r = \min(p + 1, s)$.

Theorem 4.2 (error estimates). *Let a fixed $T_h(Q)$. Let $u \in V := H_{0,0}^{1,1}(Q) \cap H^s(Q)$, with $s \geq 2$ be the solution of (2.11) and let u_h be the solution of (3.4). The solution u_h satisfies the estimates*

$$\|u - u_h\|_{h,*} \leq c_1 h^{1.5} \|u\|_{H^s(Q)}, \quad \text{for } \theta = 1, \text{ and } \kappa \sim h, \quad (4.24a)$$

$$\|u - u_h\|_{h,*} \leq c_2 h \|u\|_{H^s(Q)}, \quad \text{for } \theta \sim h, \text{ and } \kappa > h, \quad (4.24b)$$

$$\|u - u_h\|_{h,*} \leq c_3 h \|u\|_{H^s(Q)}, \quad \text{for } \theta \sim h, \text{ and } \kappa \sim h, \quad (4.24c)$$

and moreover for any $\theta > 0$,

$$\left(\|u - u_h\|_{L^2(\Sigma_T)}^2 + \kappa \|\nabla_x u - \nabla_x u_h\|_{L^2(Q)}^2 + \theta h \|\partial_t u_h^b\|_{L^2(Q)}^2 \right)^{\frac{1}{2}} \leq \frac{c_4}{\kappa} h \|u\|_{H^s(Q)}, \quad (4.25)$$

with c_i , $i = 1, 2, 3$ depending on the constants in (4.8) and in (4.20) and c_4 on the constants in (4.3) and (4.19).

Proof. The estimates (4.24) follow directly from Remark (4.1) and (4.20c). The estimate (4.25) follows from (4.3) and (4.19). \blacksquare

Remark 4.4. In realistic cases, the solutions of parabolic evolution problems may present an anisotropic regularity behavior, for example different regularities properties with respect to time and space direction. In such cases, it is more appropriate to discretize the problem using anisotropic meshes, using small mesh size in the directions where the solution is less smooth and larger mesh size in the directions where the solution is smoother, [4]. This is a topic that we will investigate in a forthcoming paper.

5 Numerical examples

In this section, we present several numerical examples for validate the theoretical estimates. Although in the analysis, we used linear polynomial spaces, next we perform tests using both linear, ($p = 1$), and second order, ($p = 2$), polynomial spaces, which are combined with the associated cubic bubble space. For all tests, we use triangular or tetrahedral mesh elements. Every example has been solved applying several mesh refinement steps with corresponding mesh

size $h_s = \frac{h_0}{2^s}$, $s = 1, 2, \dots, s = 6$. Every $T_{h_s}(Q)$ satisfies the properties mentioned in Section 3. We present tables with the asymptotic behavior of the error convergence rates r . The numerical convergence rates r have been computed by the ratio $r = \frac{\ln(e_s/e_{s+1})}{\ln(h_s/h_{s+1})}$, where the error $e_s := \|u - u_h\|_{h,*}$ is computed on $T_{h_s}(Q)$. We mention that, in the test cases, we use highly smooth solutions, i.e., $\min(p+1, \ell) = p+1$, see (4.19). We study the behavior of the rates r for $\theta = 1$ and for $\theta \sim h$. Furthermore, we investigate the behavior of r when the mesh size is close to the number of κ , and in particular, we performed tests setting $\kappa \sim h_5$. The results are displayed in tables with headline columns $\kappa \sim h_5$. Lastly, we point out that since the support of a bubble function is restricted to the interior of the element, we eliminate the the associated variable from the produced linear system by static condensation.

Example 1: $Q \subset \mathbb{R}^2$, $p = 1$. In the first example, the problem is considered in $Q = (0, 1) \times (0, 2)$. The exact solution is given by the formula

$$u(x, t) = \sin(2\pi x) \sin(\pi t). \quad (5.1)$$

The source function f is determined by (5.1). Note that $u = 0$ on Σ and $u_0 = 0$, see (2.7). In Fig. 2, we plot the exact solution on Q . We solve the problem using linear polynomials, $p = 1$. We begin by first setting $\kappa = 1$ and $\theta = 1$ and continue by setting $\theta \sim h_s$. The numerical convergence rates for the several levels of mesh refinement are presented in the first columns in Table 1. They are in very good agreement with the theoretically predicted estimates given in 4.24. We observe that the numerical solution $u_h \in V_{h,b}$ gives optimal convergence rates, i.e., the values of r are very close to one, for all the refinement steps. Next, we perform the same computations by setting $\kappa = 0.92 h_5$. The associated convergence rates are presented in the last columns in Table 1. For the case $\theta = 1$, we observe that the rates r at the last refinement steps approaching the value 1.5, which is in agreement with the predicted rates in (4.24a). Similarly, for the case $\theta \sim h_s$, the value of r are little higher than one, for the firs mesh levels. However, as we move on to the next mesh levels, the values of r are close to one, and thus are in agreement with the values predicted by the theory.

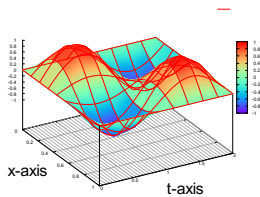


Fig. 2: Example 1: The solution u on Q .

h_s	$p = 1, \kappa = 1$		$p = 1, \kappa \sim h_5$	
$h_0/2^s$	$\theta = 1$	$\theta \sim h_s$	$\theta = 1$	$\theta \sim h_s$
Convergence rates r				
$s = 1$	1.09	1.10	0.93	1.35
$s = 2$	1.04	1.06	1.20	1.31
$s = 3$	1.13	1.11	1.35	1.14
$s = 4$	0.97	0.99	1.38	1.10
$s = 5$	1.13	1.10	1.41	1.03
$s = 6$	1.04	1.01	1.47	1.02

Table 1: Example 1: The convergence rates r .

Example 2: $Q \subset \mathbb{R}^2$, $p = 2$. In the second example, we consider the problem on $Q = (0, 1) \times (0, 1)$. The exact solution is given by the formula

$$u(x, t) = \sin(2\pi t) \sin(2\pi x). \quad (5.2)$$

The source function f is defined to match the solution in (5.2). In Fig. 3, we plot the exact solution u on a relative coarse mesh with $h = 0.25$. We solve the problem using second order, $p = 2$, polynomial space. For the first group of computations we set $\kappa = 1$, $\theta = 1$ and $\theta \sim h_s$. In the first columns in Table 2, we show the convergence rates r . As in the previous example, the values of r are approaching the value two, and confirm the theoretical predicted rates given in Theorem 4.2. We repeat the same computations setting $\kappa = 0.1$ and keeping the same values

for θ . The produced rates r are shown in last columns in Fig. 2. We observe that, for the first mesh levels, the values of r are higher than the expected values. The reason can be that the mesh size h_s for these meshes is close to the value of κ , see also the rates in third column in Table 1. Moving to the next mesh levels, we can see that the rates are approaching the expect value and are in agreement with the predicted estimates in (4.24). For the case $\theta \sim h_s$, we can see that the rates r are close to two, as it was expected.

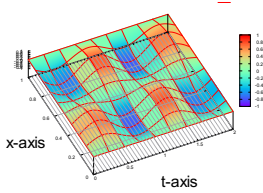


Fig. 3: Example 2: The solution u on Q

h_s	$p = 2, \kappa = 1$		$p = 2, \kappa = 0.1$	
$h_0/2^s$	$\theta = 1$	$\theta \sim h_s$	$\theta = 1$	$\theta \sim h_s$
Convergence rates r				
$s = 1$	2.10	2.70	2.28	1.75
$s = 2$	1.90	1.80	2.21	1.92
$s = 3$	1.91	1.95	2.25	2.20
$s = 4$	1.90	1.99	2.06	2.19
$s = 5$	1.93	1.96	2.09	2.11
$s = 6$	1.94	1.97	2.10	2.00

Table 2: Example 2: The convergence rates r .

Example 3: $Q \subset \mathbb{R}^3$, $p = 1$. In this third example, the problem is considered on $Q = \Omega \times (0, 1)$ with $\Omega = (0, 1)^2$. The exact solution is given by the formula

$$u(x, y, t) = (\cos(2\pi(x - y)) - \cos(2\pi(x + y))) \sin(2\pi t). \quad (5.3)$$

Note that $u = 0$ on Σ and $u_0 = 0$. The function f is determined by (5.3). In Fig. 4, we plot the contours of u for $t = 0.8$. The problem has been solved on a sequence of meshes as in the previous tests using linear polynomial space, $p = 1$. We perform similar computations as before, choosing $\kappa = 1$ and $\kappa = 0.2$. In the first columns in Table 3, we can see the values of the convergence rates r for $\kappa = 1$. We observe that the numerical solution exhibits first order convergence for both cases $\theta = 1$ and $\theta \sim h_s$. These rates are compatible with the theoretical estimates presented in Theorem 4.2. The last columns in Table 3 show the rates for $\kappa = 0.2$. For the first coarse meshes, the rates related to $\theta = 1$ are little higher than the expected. This can be explained by the fact that the magnitude of the diffusivity κ is close to the mesh sizes. The next rates related to the finer meshes are close to one and are in agreement with the theory. Also, the rates related to $\theta \sim h_s$ are optimal for linear polynomial spaces and in agreement with the theoretical predicted estimates.

Finally, we can conclude that the proposed bubble stabilization finite element scheme performs well for all the examples. The produced numerical solution gives optimal order of convergence in the $\|\cdot\|_{h,*}$ -norm, when problems with smooth solutions are solved.

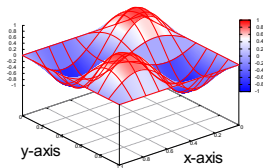


Fig. 4: Example 3: The solution u on $Q \subset \mathbb{R}^3$

h_s	$p = 1, \kappa = 1$		$p = 1, \kappa = 0.2$	
$h_0/2^s$	$\theta = 1$	$\theta \sim h$	$\theta = 1$	$\theta \sim h_s$
Convergence rates r				
$s = 1$	1.09	1.02	0.61	0.60
$s = 2$	0.90	0.90	1.38	1.26
$s = 3$	0.92	0.90	1.30	1.16
$s = 4$	0.97	0.97	1.17	1.15
$s = 5$	1.05	1.05	1.10	1.11

Table 3: Example 3: The convergence rates r .

6 Conclusions

In this article, we have proposed and analyzed a bubble stabilized space-time finite element method for solving linear parabolic evolution problems. The construction of the method was based on a space-time variational formulation of the initial PDE problem, which allows the unified space-time discretization by finite element techniques. We presented a discretization error analysis and proved that the method has optimal convergence properties, when the PDE problem has smooth solution. We showed that the optimal order of convergence is not affected by the choice of the value of the parameter θ appearing in the additional bubble stabilization terms. The theoretical findings have been verified by performing several numerical examples. A possible extension of the presented work is to combine the proposed method with time or space-time mesh adaptivity techniques.

Acknowledgements

The author wish to thank Andreas Schafelner for the additional validation of the results presented in Section 5. This work was supported by the Austrian Science Fund (FWF) under the grant NFN S117-03.

References

1. G. Akrivis and C. Makridakis. Galerkin time-stepping methods for nonlinear parabolic equations. *ESAIM: Mathematical Modelling and Numerical Analysis*, 38(2):261–289, 2004.
2. R. Andreev. Stability of sparse space-time finite element discretizations of linear parabolic evolution problems. *IMA, J. Num. Anal.*, 33(1):242–260, 2013.
3. R. Andreev. On long time integration of the heat equation. *Calcolo*, 53(1):19–34, 2016.
4. T. Apel. Interpolation of non-smooth functions on anisotropic finite element meshes. *ESAIM: Mathematical Modelling and Numerical Analysis*, 33(6):1149–1185.
5. I. Babuška and T. Janik. The h-p version of the finite element method for parabolic equations. Part I. the p-version in time. *Numerical Methods for Partial Differential Equations*, 5(4):363–399, 1989.
6. I. Babuška and T. Janik. The h-p version of the finite element method for parabolic equations. II. the h-p version in time. *Numerical Methods for Partial Differential Equations*, 6(4):343–369, 1990.
7. C. Baiocchi, F. Brezzi, and L. P. Franca. Virtual bubbles and Galerkin-least-squares type methods (Ga.L.S.). *Computer Methods in Applied Mechanics and Engineering*, 105(1):125 – 141, 1993.
8. S.C. Brenner and L. R. Scott. *The mathematical Theory of Finite Element Methods*, volume 15 of *Texts in Applied Mathematics*. Springer-Verlag New York, third Edition edition, 2008.
9. F. Brezzi, M.-O. Bristeau, L. P. Franca, M. Mallet, and G. Rogé. A relationship between stabilized finite element methods and the Galerkin method with bubble functions. *Computer Methods in Applied Mechanics and Engineering*, 96(1):117 – 129, 1992.
10. N. Chegini and R. Stevenson. Adaptive wavelet schemes for parabolic problems:sparsematrices and numerical results. *SIAM J. Numer. Anal.*, 49:182–212, 2011.
11. P. G. Ciarlet. *The Finite Element Method for Elliptic Problems*. Studies in Mathematics and its Applications. North Holland Publishing Company, 1978.
12. K. Eriksson and C. Johnson. Error estimates and automatic time step control for nonlinear parabolic problems I. *SIAM J. Numer. Anal.*, 24:12–23, 1987.
13. K. Eriksson and C. Johnson. Adaptive finite element methods for parabolic problems IV: Nonlinear problems. *SIAM J. Numer. Anal.*, 32(6):1729–1749, 1995.
14. K. Eriksson and C. Johnson. Adaptive finite element methods for parabolic problems V: Long-time integration. *SIAM J. Numer. Anal.*, 32(6):1750–1763, 1995.
15. K. Eriksson, C. Johnson, and V. Thomeé. Time discretization of parabolic problems by the Discontinuous Galerkin Method. *RAIRO Modél. Math. Anal. Numér.*, 19:611–643, 1985.
16. A. Ern and J.-L. Guermond. *Theory and Practice of Finite Elements*, volume 159 of *Applied Mathematical Sciences*. Springer-Verlag New York, 2004.
17. J. L. Guermond. Stabilization of Galerkin approximations of transport equations by subgrid modeling. *ESAIM: M2AN*, 33(6):1293–1316, 1999.
18. J. L. Guermond. Subgrid stabilization of galerkin approximations of linear monotone operators. *IMA Journal of Numerical Analysis*, 21(1):165, 2001.
19. P. Hansbo. The characteristic streamline diffusion method for the time-dependent incompressible Navier-Stokes equations. *Computer Methods in Applied Mechanics and Engineering*, 99(2-3):171–186, 1992.
20. P. Hansbo. Space-time oriented streamline diffusion methods for non-linear conservation laws in one dimension. *Communications in Numerical Methods in Engineering*, 10(3):203–215, 1994.

21. T. J.R. Hughes and G. M. Hulbert. Space-time finite element methods for elastodynamics:formulations and error estiamtes. *Comput. Methods Appl. Mech. Engrg.*, 66:339–363, 1988.
22. C. Johnson. *Numerical Solution of Partial Differential Equations by the Finite Element Method*. Cambridge University Press, 1988.
23. O. A. Ladyzhenskaya. *The Boundary Value Problems of Mathematical Physics*, volume 49 of *Applied Mathematical Sciences Series*. Springer New York, 1985.
24. U. Langer, S.E. Moore, and M. Neumüller. Space-time isogeometric analysis of parabolic evolution problems. *Computer methods in applied mechanics and engineering*, 306:342–363, 2016.
25. U. Langer, M. Neumüller, and I.Toulopoulos. Multipatch space-time isogeometric analysis of parabolic diffusion problems. In I. Lirkov and S. Margenov, editors, *Large-Scale Scientific Computing*, Lecture Notes in Computer Science, Heidelberg, 2017. Springer. accepted for publication. Also available as RICAM report Nb 2017-18 at <https://www.ricam.oeaw.ac.at/publications/ricam-reports/>.
26. A. Quarteroni and A. Valli. *Numerical approximation of partial differential equations*, volume 23. Springer-Verlag Berlin Heidelberg, 1994.
27. C. Schwab and R. Stevenson. Space-time adaptive wavelet methods for parabolic evolution problems. *Math. Comp.*, 78:1293–1318, 2009.
28. O. Steinbach. Space-time finite element methods for parabolic problems. *Comp. Methods Appl. Math.*, 15(4):551–556, 2015.
29. V. Thomeé. *Galerkin finite element methods for parabolic problems*, volume 25 of *Springer Series in Computational Mathematics*. Springer-Verlag Berlin Heidelberg, 2006.
30. E. Zeidler. *Nonlinear functional analysis and its applications,II/A: Linear monotone operators*. Springer-Verlag New York, 1990.